

Molecular species composition of polar lipids from two microalgae *Nitzschia palea* and *Scenedesmus costatus* using HPLC-ESI-MS/MS

Nicolas Mazzella¹, Mariem Fadhlaoui², Aurélie Moreira¹ and Soizic Morin¹

¹INRAE, UR EABX, Cestas, France

²INRS-EET, Québec, Canada

ABSTRACT

This study examines the polar lipid profiles of two freshwater algae, *Scenedesmus costatus* and *Nitzschia palea*. HILIC-ESI-MS/MS analysis was used to determine and quantify the major phospholipids and glycolipids, as well as their relative molecular species, extracted from the two microalgal cultures. Glycolipids were eluted first, followed by phospholipids partially co-eluting with a sulfoglycolipid. The fragmentation pattern in the negative ionization mode for galactolipids was studied, revealing the stereospecific distribution of fatty acids on the glycerol backbone. Green algae frequently include 18:3 fatty acid in both phospholipids and galactolipids, while monogalactosyldiacylglycerol (MGDG) and digalactosyldiacylglycerol (DGDG) were more saturated and contained shorter acyls. The diatom phospholipids contained mainly molecular species with saturated or monounsaturated fatty acids, while MGDG and DGDG exhibited a higher proportion of polyunsaturated fatty acids, such as the unique and abundant MGDG (20:5/20:2).

Subjects Hyphenated Techniques, Mass Spectrometry, Omics Technologies

Keywords Glycolipids, Phospholipids, Fatty acids, Mass spectrometry, Diatoms, Chlorophyta, Freshwater

Submitted 4 May 2023
Accepted 26 July 2023
Published 11 September 2023

Corresponding author
Nicolas Mazzella,
nicolas.mazzella@inrae.fr,
n.mazzelladibosco@gmail.com

Academic editor
Young Jin Lee

Additional Information and
Declarations can be found on
page 15

DOI 10.7717/peerj-achem.27

© Copyright
2023 Mazzella et al.

Distributed under
Creative Commons CC-BY 4.0

OPEN ACCESS

INTRODUCTION

In rivers, periphytic microalgae (*i.e.*, attached to any substrate, either mineral or organic) are often at the bottom of the trophic chain, and plays an important resource for higher trophic level taxa. They typically arise in the form of a biofilm., where organisms from several kingdoms cohabit: besides microalgae, bacteria, fungi and pluricellular micro-eukaryotes are embedded together in a matrix of extracellular polymeric substances. Many herbivores consume biofilms as a primary food source and biofilms, or more specifically their algal component, are receiving increasing attention because they are a source of essential fatty acids for higher consumers (*Taipale et al., 2013; Brett & Müller-Navarra, 1997*). They can be used to describe relationships within the aquatic food webs (*Kelly & Scheibling, 2012*) and are often used as indicators of trophic quality in ecosystems. It has long been shown that total fatty acid profiles differ between groups of algae. In freshwater biofilms, which are often dominated by diatoms and chlorophytes, the specific origin influences the overall composition of the food available for consumers, making it a crucial driver of the health

and stability of aquatic food chains. According to *Arts, Ackman & Holub (2001)*, both ω 3 eicosapentaenoic acid (EPA, 20:5*n*-3) and docosahexaenoic acid (DHA, 22:6), and the ω 6 arachidonic acid (ARA, 20:4*n*-6) are key fatty acids for zooplankton and fish. Freshwater diatoms are also rich in palmitoleic acid (16:1*n*-7), palmitic acid (16:0), and myristic acid (14:0). Most importantly, diatoms are an important source of fatty acids essential for higher consumers, especially EPA and ARA (*Taipale et al., 2013*), and also contain low but significant amounts of DHA (*Demilly et al., 2019*). In contrast, the major fatty acids in chlorophytes are α -linolenic acid (ALA, 18:3*n*-3), palmitic acid, oleic acid (18:1*n*-9), and α -linoleic acid (LIN, 18:2*n*-6). Lastly, phosphatidylglycerol and some peculiar galactolipids are the main component of thylakoid membranes in all microalgae (*Mizusawa & Wada, 2012; Da Costa et al., 2016; Guschina & Harwood, 2006*), and especially their respective fatty acid constituent (*i.e.*, molecular species) were partly investigated for diatom and chlorophyte species so far. Actually, with the exception of a few marine species, lipid algal metabolism has been little studied to date, and we still have limited knowledge of the biochemical processes underlying the synthesis or plasticity of the major lipid classes (*Cutignano et al., 2016; Li et al., 2018*).

This is within this framework that we are interested in the analysis of polar lipids of two freshwater microalgae (*Nitzschia palea* and *Scenedesmus costatus*). On the one hand, we aim to characterize the main molecular species associated with both glycolipids and phospholipids, including some fragmentation patterns in mass spectrometry. On the other hand, we aim to quantify each of these compounds. The aim is here to provide a methodology, and then to enlighten the typical polar lipidome profile for both “model” diatom and green algae.

MATERIALS & METHODS

Chemicals and materials

The following polar lipid standards were purchased from Avanti Polar Lipids: 1-palmitoyl-2-oleoyl-*sn*-glycero-3-phosphocholine or PC (16:0/18:1) (850457), 1-palmitoyl-2-oleoyl-*sn*-glycero-3-phosphoethanolamine or PE (16:0/18:1) (850757), 1-palmitoyl-2-oleoyl-*sn*-glycero-3-phospho-(1'-*rac*-glycerol) or PG (16:0/18:1) (840457), 1,2-diheptadecanoyl-*sn*-glycero-3-phosphocholine or PC (17:0/17:0) (850360), 1,2-diheptadecanoyl-*sn*-glycero-3-phosphoethanolamine or PE (17:0/17:0) (830756), 1,2-dipentadecanoyl-*sn*-glycero-3-phosphoethanolamine or PE (15:0/15:0) (850704), and 1,2-diheptadecanoyl-*sn*-glycero-3-phospho-(1'-*rac*-glycerol) or PG (17:0/17:0) (830456), L- α -phosphatidylserine (Soy, 99%) (sodium salt) (870336) for the phospholipid standards, and monogalactosyldiacylglycerol (840523), digalactosyldiacylglycerol (840524) and sulfoquinovosyldiacylglycerol (840525) from plant extracts as glycolipid standards. Ammonium acetate (LiChropur) were provided by Sigma-Aldrich. Acetonitrile, methanol (MeOH) tert-Butyl methyl ether (MTBE) and isopropanol HPLC grades were purchased from Biosolve Chimie, France. Ultrapure water (UPW) was obtained from Direct-Q[®] Water Purification System (Merck Millipore, Burlington, MA, USA).

Algal cultures

The algal cultures were purchased at the Thonon Culture Collection (*Rimet et al., 2018*) under culture references TCC 583 (*i.e.*, the diatom *Nitzschia palea*) and TCC 744 (*i.e.*, the chlorophyte *Scenedesmus costatus*). Both taxa were selected to be common microalgal species in freshwater environments, originated from rivers of the French metropolitan territory. Indeed, the diatom was isolated from the river la Chiers at Longlaville (Eastern France), and the chlorophyte from the stream Foron, a tributary of Lake Léman (France/Switzerland). The algal cultures were incubated in thermoregulated chambers (temperature: 18 °C, light:dark cycle: 16 h:8 h, photosynthetic active radiation reaching the cultures under light conditions: 65 $\mu\text{mol photons}\cdot\text{sec}^{-1}$), in 100-mL Erlenmeyer flask for two exponential growth cycles of seven days before the experiment began. After the two growth cycles aiming at acclimating and synchronizing the cultures, 10 mL of diatom culture (*N. palea*) were put into 60 mL of modified Dauta medium (*Dauta, 1982*) to reach an initial cell density of $297 \pm 75 \text{ cell } \mu\text{L}^{-1}$. Five replicate cultures were prepared and placed in the thermoregulated chambers under the conditions described above for pre-exposure. In the case of the chlorophyte *S. costatus*, 20 mL of culture and 50 mL of modified Dauta medium (*Dauta, 1982*) were used to obtain an initial cell density of $1,834 \pm 144 \text{ cell } \mu\text{L}^{-1}$. Cultures were performed in three independent replicates, in the thermoregulated chambers under the same conditions as *N. palea*.

Lipid extraction

Portions of the following method sections were previously published as part of a preprint (*Mazzella et al., 2023a*). Briefly, 150 mg of microbeads (0.5 mm diameter) were added to 2 mL microtubes along with 10–20 mg (dry mass) of a microalgae culture, which was weighed on a Mettler Toledo NS204S precision balance. Prior to extraction, a 50 μL solution of PE (15:0/15:0) at 100 ng L^{-1} was added as a surrogate. The extraction method was adapted from *Matyash et al. (2008)* and consisted of adding 1 mL MTBE:MeOH (3:1, v/v) followed by 650 μL UPW:MeOH (3:1, v/v). A MP Biomedicals FastPrep-24 5G (three cycles of 15 s) allowed homogenization of the solution and mechanical lysis of the sample by the microbeads, thus releasing the analytes from the sample. The upper lipophilic phase (MTBE) was separated from the lower hydrophilic phase (UPW and MeOH) by centrifugation at 12,000 rpm (*i.e.*, 16,000 g). At this point, 600 μL of the lipophilic phase was collected. After adding 700 μL of MTBE:MeOH (3:1, v/v) and 455 μL of UPW:MeOH (3:1, v/v) to the remaining hydrophilic phases, a second extraction (three cycles 15 s) was performed. The supernatant was collected after centrifugation and added to the previous one. Only the collected MTBE phases (about 1.1 mL) were kept for polar lipid analysis. To avoid any enzymatic activity that could contribute to the degradation of the lipid extracts, the entire operation was performed on ice, and butylated hydroxytoluene (BHT, 0.01% (w/v)) was initially added as an antioxidant. A procedural solvent blank was extracted in addition to the samples to confirm that no contamination occurred during the extraction step. All the extracts were stored in a $-80 \text{ }^\circ\text{C}$ freezer. Prior to hydrophilic interaction chromatography coupled to tandem mass spectrometry (HILIC-ESI-MS/MS) analysis, 50 μL of internal standards (PC, PG, and PE (17:0/17:0)) were added to each sample at a

concentration of 33.3 ng L^{-1} . MTBE was evaporated with a stream of N_2 and then diluted with an appropriate volume of isopropanol (typically 250 to 1,000 μL).

HILIC-ESI-MS/MS analysis

Lipid extracts were analyzed with a Dionex Ultimate 3000 HPLC (Thermo Fisher Scientific, Illkirch-Graffenstaden, France). An API 2000 triple quadrupole mass spectrometer (Sciex, Les Ulis, France) was used for detection. Chromatographic separation of both glycolipids and phospholipids was performed on a Luna NH_2 HILIC (3 μm , $100 \times 2 \text{ mm}$) with a Security Guard cartridge NH_2 ($4 \times 2.0 \text{ mm}$). The injection volume and temperature column were set to 20 μL and 40 $^\circ\text{C}$, respectively. The chromatographic separation conditions were reported in Table S1, a final pH value of 6.8 was retained for the ammonium acetate buffer and the flow rate was kept constant at 400 $\mu\text{L min}^{-1}$. Further details on initial method optimization and performances related to phospholipid HILIC separation can be found in Mazzella *et al.* (2023b). Quantitation of phosphatidylcholine (PC), phosphatidylethanolamine (PE) and phosphatidylglycerol (PG) were respectively carried out with PC (16:0/18:1), PE (16:0/18:1), PG (16:0/18:1). Quantitation of glycolipids was carried out with MGDG (16:3_18:3) (63% of the total MGDG standard), DGDG (18:3/18:3) (22% of the total MGDG standard), and SQDG (34:3) (78% of the total SQDG standard). The internal standards utilized were PC (17:0/17:0) for PC phospholipids, PE (17:0/17:0) for PE phospholipids and both MGDG and DGDG glycolipids, and PG (17:0/17:0) for PG phospholipids and SQDG glycolipids. Calibrations curves are provided as (Fig. S2). For glycolipids, a quadratic model was used for the data fitting, while a linear regression was generally used for phospholipids. The limits of quantification for phospholipids and glycolipids are provided in Table S2, they are finally expressed as nmol mg^{-1} (dry weight) since a typical sample of 10 mg of culture is considered for the initial extraction step. Instrumental quantification limits, initially expressed in $\mu\text{g mL}^{-1}$, were determined with signal-to-noise ratios ≥ 10 . Additionally, PE (15:0/15:0) was used as surrogate for the whole extracting procedure, with a typical recovery of $102 \pm 23\%$ ($n = 10$) (Mazzella *et al.*, 2023b). The mass spectrometry was operated at unit resolution and further parameters are reported in Table S3. Multiple-reaction monitoring (MRM) transitions for each molecular species of PC, PG, PE, MGDG, DGDG and SQDG are provided in Table S4. This HILIC-ESI-MS/MS method was adapted from a previous work (Mazzella *et al.*, 2023b); however, we have here selected the molecular species representative of microalgae, and thus reduced the number of multiple reaction monitoring (MRM) transitions followed during the two acquisition periods (Table S4). With the exception of SQDG, It was possible to determine the *sn-1/sn-2* ratio for each molecular species of interest by evaluating the relative abundances of the ions corresponding to the two acyl chains.

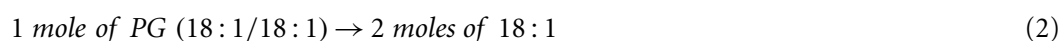
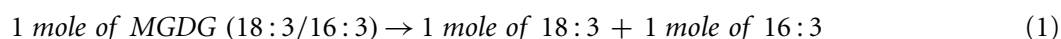
Phospholipid and glycolipid nomenclatures

Polar glycerolipids are constituted of a glycerol backbone esterified by two fatty acids on the *sn-1* and *sn-2* positions. The moiety linked to the *sn-3* position refers to the polar head group (*e.g.*, *sn*-phospho-3-glycerol for the PG, a β -D-galactosyl group for MGDG). Each polar head group defines a phospholipid or glycolipid class, and each

class can be divided into several molecular species according to the fatty acyl chain composition and distribution. Polar glycerolipids are abbreviated as follows: when the fatty acyl chain structures are resolved but the *sn*-1 and *sn*-2 positions remain unclear, then the phospholipids or glycolipids are designated PL (C:*n* _C:*n*), with C referring to the sum of the number of carbon atoms and *n* to the number of double bonds for each fatty acyl chain. When the acyl chain composition and distribution are known, then the phospholipids are noted as PL (C:*n*-1/C:*n*-2), where C:*n*-1 and C:*n*-2 correspond to the fatty acids linked to *sn*-1 and *sn*-2 positions, respectively (e.g., PG (16:0/18:1) for 1-palmitoyl-2-oleoyl-*sn*-glycero-3-phospho-rac-1-glycerol).

Conversion of phospholipids and glycolipids in fatty acid equivalents

Following the analysis of the different classes of polar lipids, and having access to the molecular species within each class, it is then possible to deduce the different fatty acids from the acyl chains determined before. To this purpose, each mole of each molecular species was converted into its fatty acid equivalent.



Equation (1) illustrates the case where the acyl chains are asymmetric (*i.e.*, the fatty acid at *sn*-1 is different from that at *sn*-2), while Eq. (2) corresponds to the other possible case (*i.e.*, the presence of two fatty acids with both the same numbers of carbons and unsaturations).

RESULTS AND DISCUSSION

Portions of this section were previously published as part of a preprint (Mazzella *et al.*, 2023a). From a HILIC-ESI-MS/MS method originally developed for phospholipid analysis (Mazzella *et al.*, 2023b), we added the MRM transitions for three classes of glycolipids commonly observed in microalgae (Li-Beisson *et al.*, 2019; Zulu *et al.*, 2018; Alonso *et al.*, 1998): monogalactosyldiacylglycerol (MGDG), digalactosyldiacylglycerol (DGDG) and sulfoquinovosyldiacylglycerol (SQDG). Figure 1 shows the elution orders for the major phospholipids (PC, PE, and PG), as well as the main glycolipids (MGDG, DGDG, and SQDG) obtained from the green algal culture extract. MGDG was eluted first in our conditions, followed by the DGDG around 3.1 min. Finally, it was SQDG that was co-eluted with PG at 6.4 min (Table S2). The absence of any quantifiable amount of phosphatidylinositol (PI) or phosphatidylserine (PS) was uncovered in a first screening of both *N. palea* and *S. costatus* extracts for five phospholipid classes, as well as all possible related molecular species (Mazzella *et al.*, 2023b). This result appeared as consistent, since PI, with both PC and PE, is mainly observed in dinoflagellates like *Schizochytrium* sp (Li *et al.*, 2016). Afterwards, in addition to the observation obtained with our initial screening (Mazzella *et al.*, 2023b) for both *S. costatus* and *N. palea*, the number of MRM transitions followed at the same time for the compounds has been reduced (Table S4). Actually, these transitions have been selected with respect to the molecular species expected

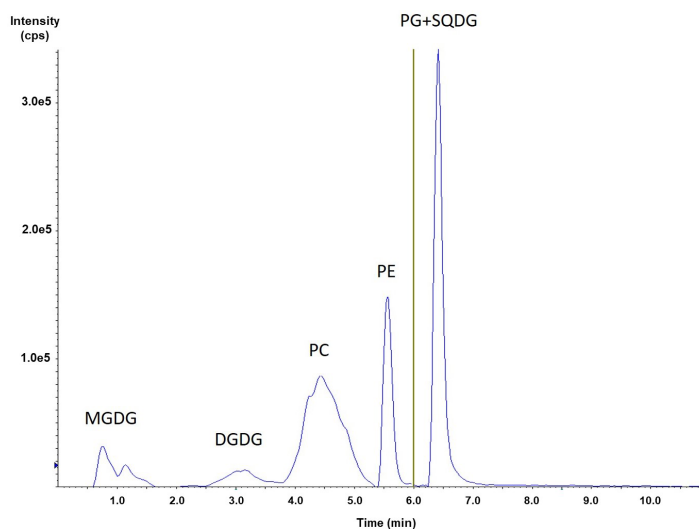


Figure 1 HILIC-ESI-MS/MS analysis of a phospholipid and glycolipids extracted from *S. costatus*.

Full-size [DOI: 10.7717/peerj.chem.27/fig-1](https://doi.org/10.7717/peerj.chem.27/fig-1)

for various microalgae (green algae, cyanobacteria, and diatoms), as well as those reported in several previous studies involving lipidomics (Mazzella et al., 2023b; Li-Beisson et al., 2019; Zulu et al., 2018; Jouhet et al., 2017; Coniglio et al., 2021; Yongmanitchai & Ward, 1993; Degraeve-Guilbault et al., 2017). With the exception of SQDG, this enabled the consideration of two MRM transitions for each analyte and allowed here the determination of the *sn*-1 and *sn*-2 locations of the acyl chains. However, in order to consider the different MRM transitions associated with each molecular species, it was necessary to determine the likely fragmentation obtained in negative electrospray ionization for such glycolipids.

MGDG fragmentation pathways

Low-energy collisionally activated dissociation with tandem quadrupole mass spectrometry previously allowed structural characterization of glycerophospholipids, especially in negative ionization mode (Hsu & Turk, 2009). Regarding glyceroglycolipids, some studies have focused on the structural elucidation, and thus the determination of fragmentation pathways from positive electrospray ionization mode (Yingbo et al., 2021; Tatituri et al., 2012). In our case, we focused more precisely on the negative ionization, and the subsequent fragmentation, obtained from a monogalactosyldiacylglycerol standard like MGDG (18:3/16:3) (the fragmentation of DGDG molecular species, not showed here, being similar). The left part of Fig. 2 exhibited the fragments obtained in product scan mode from m/z 745.8, which corresponds to MGDG (18:3/16:3), as a deprotonated molecule $[M-H]^-$, while the right parts correspond to the precursors determined from the product ions m/z 277.5 and 249.3. Herrero et al. (2007) have previously observed fragments with m/z 277 ratio, and it was attributed to γ -linolenic acid (18:3n-6) from a MGDG molecular

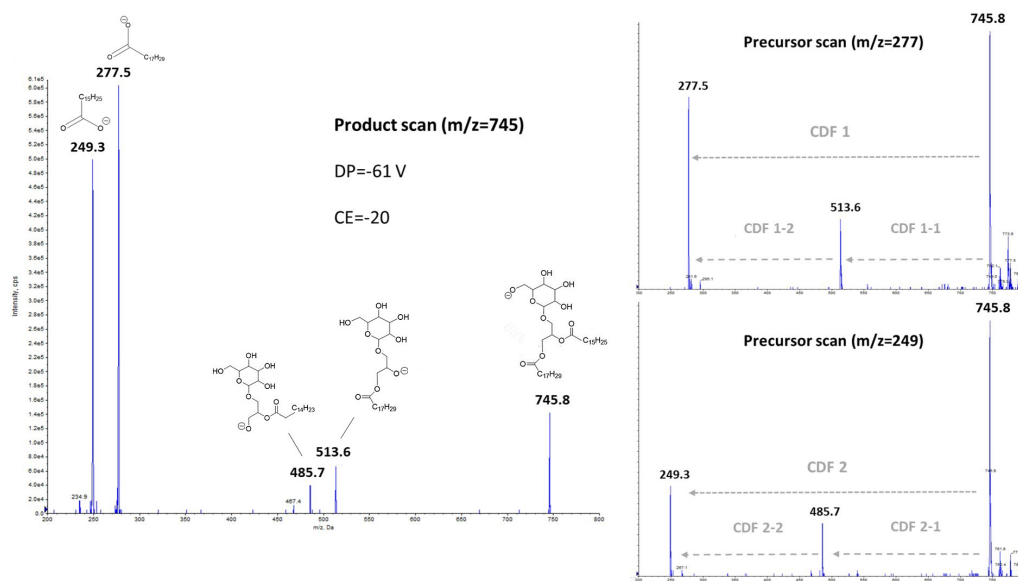


Figure 2 Negative ionization and collision-induced dissociation of MGDG (18:3/16:3), with either product scanning from m/z 745.8 (left part) or precursor scanning for m/z 277.5 and m/z 249.3 ions (right part).

Full-size DOI: 10.7717/peerj.chem.27/fig-2

species in their study. It should be noted that in the case of HPLC-MS/MS analyses, the m/z 277 ratio corresponds more generally to any deprotonated 18:3 isomers.

To explain these observations, it can be assumed that mechanisms such as charge-driven fragmentation (CDF) processes would occur for glycolipids, as for phospholipids during a negative ionization mode (Mazzella *et al.*, 2005). Due to the intensity of the two carboxylate ions at m/z 249.3 and m/z 277.5 formed from the parent ion at m/z 745.8 (Fig. 2), a CDF-type mechanism is mainly suspected. In Fig. 3, we proposed two possible pathways with a CDF 1 mechanism inducing the formation of the $R_1\text{COO}^-$ ion characterized by a m/z 277.5 ratio, and then another CDF 2 mechanism resulting in the formation of the $R_1\text{COO}^-$ ion characterized by a m/z 249.3 ratio. The dominance of these two CDF mechanisms was confirmed by precursor scanning, which revealed the prevailing m/z 745.8 ratio that also corresponds to the pseudo-molecular ion $[\text{M}-\text{H}]^-$. In this suggested mechanism, we have assumed an initial localization of the negative charge with the formation of a likely ‘alkoxide’ ion.

In our case, a second mechanism could also be taken into account with an initial neutral loss of the fatty acyl chain as a ketene (*i.e.*, $\text{R}_2\text{CH}=\text{C}=\text{O}$) from *sn*-2 position (CDF 1-1). It can be proposed that the deprotonation at the α carbon on the acyl chain affords an ‘enolate’ ion (Fournier *et al.*, 1993) that immediately undergoes a C-O bond releasing the $\text{C}_{14}\text{H}_{23}-\text{CH}=\text{C}=\text{O}$ neutral, and then affording m/z 513.6 (Fig. 4) ion with a negatively charged oxygen atom (*i.e.*, alkoxide ion). A following CDF process (*i.e.*, CDF 1-2) may produce the release of the fatty acyl chain located at *sn*-1 position, with the occurrence of ion at m/z 277.5. The alternative pathway consists in the neutral loss of fatty acid a ketene (*i.e.*, $\text{R}_1\text{CH}=\text{C}=\text{O}$) from *sn*-1 position (CDF 2-1), and then the final formation

MGDG (18:3/16:3)

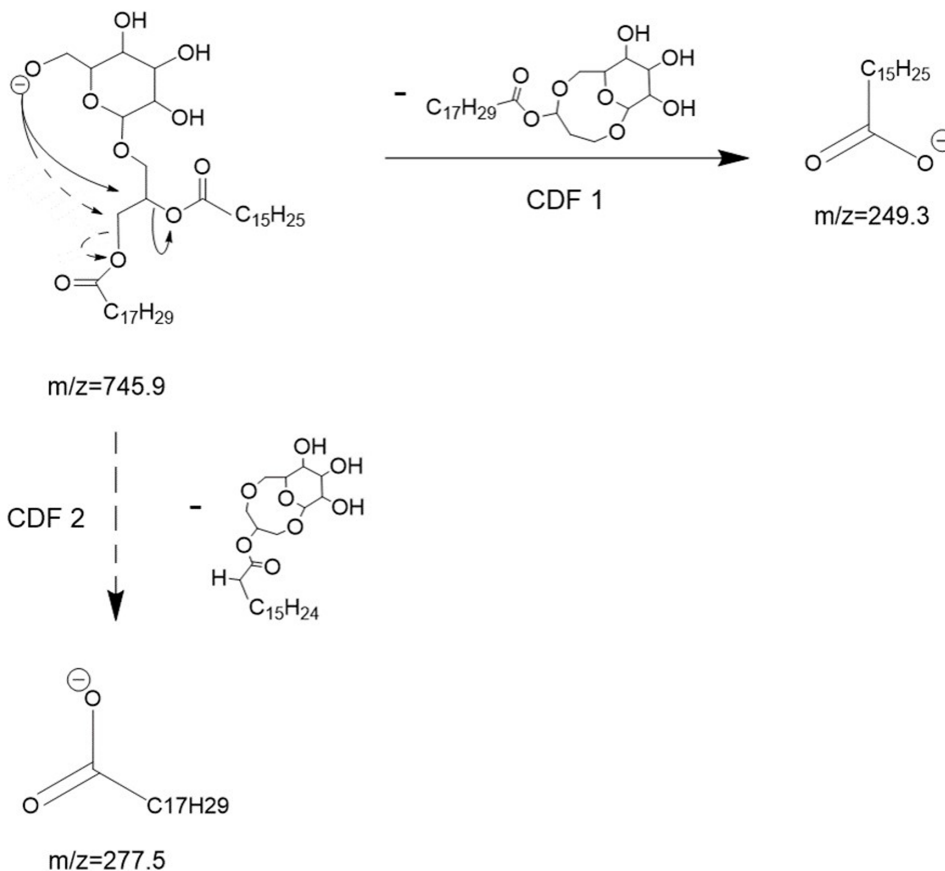


Figure 3 Proposed collision-induced dissociation (CID) pathways of MGDG (18:3/16:3) after electrospray ionization showing the direct formation of $[R_1COO]^-$ and $[R_2COO]^-$ ions via CDF 1 and 2 processes, respectively.

Full-size DOI: 10.7717/peerj.chem.27/fig-3

of the m/z 249.3 ion (CDF 2-2). In the Fig. 4, for readability reasons, only a CDF 1-1 pathway, preceding the CDF 1-2 step, with a proton transfer rearrangement was shown. The suggested alternative CDF 2-1 and 2-2 pathways would follow the same principle. Lastly, two other mechanisms might result in the neutral loss of acyl chains as protonated acids (*i.e.*, R_1COOH or R_2COOH). In that case, we should observe ions at m/z 495.5 and m/z 467.5, but these were hardly visible and anyway much less intense than the m/z 513.6 and m/z 485.7 ions for collision energies tested between 10 and 30 eV.

In this study, whatever the mechanisms and pathways involved, it appears that the most intense product ion corresponds to the fatty acyl chain located at *sn*-1 position, allowing the determination of stereospecific distribution of subsequent fatty acids on the glycerol backbone. Such a result comes into sight as inverted in comparison to the usual negative fragmentation and the latterly observed *sn*-1/*sn*-2 ratio for phosphatidylglycerol, and other phospholipids in general (Hsu & Turk, 2009; Mazzella *et al.*, 2004; Hsu & Turk,

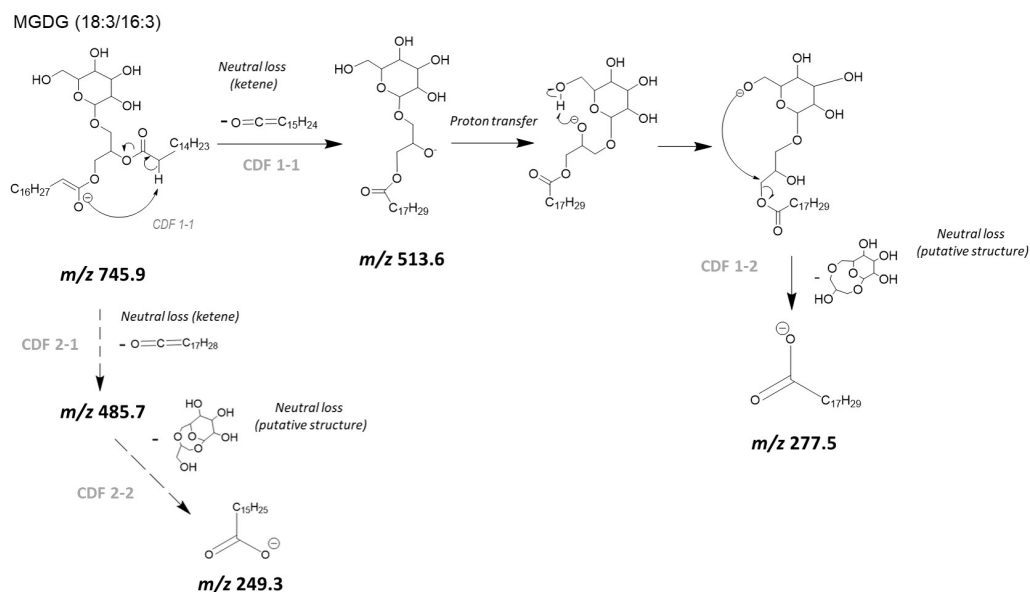


Figure 4 Proposed collision-induced dissociation (CID) pathways of MGDG (18:3/16:3) after electrospray ionization showing the likely successive formation of $[M - H - R_2CH = C = O]^-$ and $[R_1COO]^-$ ions (CDF 2-1, and then CDF).

Full-size DOI: 10.7717/peerj.chem.27/fig-4

2001; Pi, Wu & Feng, 2016; Huang et al., 2019; Hsu & Turk, 2000). Such a property has been employed here in order to determine the likely regiochemistry of the two acyl chains within the molecular species of MGDG and DGDG, in addition to those associated with PG, PE and PC. This is illustrated by ion ratios observed for the three pairs of molecular species (*i.e.*, possible isomers) of PG (16:0/16:1) and PG (16:1/16:0), PE (16:1/18:1) and PE (18:1/16:1), and DGDG (20:5/16:1) and DGDG (16:1/20:5) (Fig. S1). For instance, the higher intensity of the m/z 253 ratio over the m/z 255 ratio, both obtained from the m/z 719 ion, indicates the preferential occurrence of the PG (16:0/16:1) regioisomer in that case. Conversely, the higher intensity of the m/z 301 ratio over the m/z 253 ratio, both originating from the m/z 935 ion, should mainly correspond to the DGDG (20:5/16:1) conformation.

Intact polar lipids of two microalgae extracts

Phospholipid and glycolipid molecular species of *N. palea* and *S. costatus*

The upper parts of Tables 1 and 2 outline the two microalgae the different molecular species within the detected phospholipids (PE, PG and PC), as well as among the two galactolipids (MGDG and DGDG). In the case of SQDG, fragmentation in negative mode mainly allowed the observation of the characteristic ion at m/z 225 (Hsu & Turk, 2009; Mazzella et al., 2007), and not the couple of ions associated with losses of acyl chains. The expected neutral loss (Zulfiqar et al., 2003) (*e.g.*, m/z 537.4 with a precursor ion m/z 793.5 corresponding to the neutral loss of a 16:0 fatty acid) was barely visible in our case, regardless of the collision energy applied. It was therefore not possible in this case, unlike the other glycerolipids investigated here, to determine the fatty acid composition, resulting

in a general SQDG-type notation ($\sum C: \sum n$), with $\sum C$ the total number of carbon and $\sum n$ the total number of double bonds of the two fatty acids, respectively. Within the phospholipids of *N. palea* (Table 1), it is remarkable that PE and PG contain mainly molecular species with saturated (SFAs) or monounsaturated (MUFAs) fatty acids like 16:0, 16:1, and 18:1. PC differs with many more polyunsaturated fatty acids (PUFAs) such as 20:5 and 22:6. This is also the case for MGDG and DGDG, with the observation of the unique and very abundant MGDG (20:5/20:2) with nearly 2.66 nmol mg⁻¹, followed by the four molecular species of DGDG of which three contain 20:5. In accordance with the description in other previous works compounds (Cutignano *et al.*, 2016; Jouhet *et al.*, 2017; Yongmanitchai & Ward, 1993), it should be noted that fatty acids with 16 carbons along with PUFAs, when present, are preferentially positioned in *sn*-2 in this study, reflecting the prokaryotic pathway in the original synthesis of these acylglycerol lipids. Finally, the predominant species of SQDG (32:1) probably corresponds to a combination of 16:0 and 16:1, although this cannot be confirmed analytically due to specific CID fragmentation in our case, as mentioned above.

As reported in Table 2, concerning the green algae (*S. costatus*), we noted, unlike the diatom strain, the frequent presence of 18:3, both among phospholipids and galactolipids, while 20:5 is absent this time. We also find some 16:4 in some molecular species of both MGDG and DGDG. The characteristic MGDG species in most green algae are actually (18:3/16:4), and to a less amount (18:3/16:3), which may be produced by sequential desaturation of MGDG (18:1/16:0) as shown for *Chlamydomonas* or *Dunaliella* (Giroud, Gerber & Eichenberger, 1988; Sanina, Goncharova & Kostetsky, 2004). DGDG are somewhat more saturated than MGDG, and contains mainly 18:1, 18:2 or 18:3 at *sn*-1 and the shorter 16:0, 16:1, 16:2 and 16:3 moieties at *sn*-2. In addition, the preferential occurrence of 16:3 and 16:4 over 18:3 PUFAs in DGDG compared to PE, PC and PG molecular species was also revealed by lipid content and fatty acid composition of the green alga *Scenedesmus obliquus* (Choi *et al.*, 1987) determined with different methodology and analytical techniques (*i.e.*, thin layer and gas liquid chromatography). Consequently, our results appeared to be consistent with these general patterns reported for some *Chlorophyceae*.

Besides, in the case of PG, MGDG and DGDG, when a PUFA is associated with either a MUFA or SFA, it is then mostly found in the *sn*-1 position. The opposite pattern appeared for PE and PC, indicating a likely biosynthesis in the endoplasmic reticulum for these two phospholipids (Yongmanitchai & Ward, 1993).

Polar lipid classes of *N. palea* and *S. costatus*

The bottom of Table 1 as well as the bottom of Table 2 summarize the sums of each molecular species, and with these sums, it can be possible to deduce the polar lipid classes for each of the two microalgae. In both cases, MGDG and SQDG are predominant among the glycolipids, followed by PG in the phospholipids from thylakoids. Glycolipids including MGDG, DGDG and SQDG are prevalent in the plant kingdom, representing around 70–85% of membrane lipids in chloroplasts (Block *et al.*, 1983). It is well known that thylakoid membrane of chloroplasts is unique in lipid composition, with mono-

Table 1 Amounts of phospholipid and glycolipid molecular species extracted from *N. palea* ($n = 5$). Molecular weights, standard deviations (SD) and relative standard deviations (% RSD) are also indicated.

Molecular species	MW (Da) ^a	Mean (nmol mg ⁻¹) ^b	SD	% RSD
PE(16:0/16:1)	689	0.60	0.211	35%
PE(16:1/16:1)	687	0.76	0.350	46%
PE(18:1/16:1)	715	0.37	0.148	40%
PG(16:1/14:0)	692	0.13	0.057	46%
PG(16:0/16:1)	720	0.56	0.213	38%
PG(16:1/16:1)	718	0.27	0.098	37%
PG(18:1/16:1)	746	0.38	0.155	41%
PG(20:5/18:1)	794	0.10	0.000	0%
PC(20:5/16:1)	778	0.15	0.125	83%
PC(20:5/22:6)	852	0.11	0.012	11%
MGDG(20:5/20:2)	828	2.66	1.417	53%
DGDG(16:1/16:1)	916	0.13	0.032	24%
DGDG(20:5/16:1)	936	0.23	0.090	40%
DGDG(20:5/16:2)	934	0.19	0.097	50%
DGDG(20:5/20:0)	994	0.15	0.057	38%
SQDG(30:1)	765	0.06	0.012	20%
SQDG(32:0)	795	0.08	0.014	17%
SQDG(32:1)	793	1.15	0.351	31%
SQDG(32:2)	791	0.16	0.035	22%
SQDG(34:5)	813	0.06	0.010	17%
SQDG(36:4)	843	0.05	0.007	14%
SQDG(36:5)	841	0.13	0.025	19%
SQDG(42:5)	925	0.05	0.008	15%
∑ PE		1.73	0.692	40%
∑ PG		1.43	0.497	35%
∑ PC		0.26	0.137	53%
∑ MGDG		2.66	1.417	53%
∑ DGDG		0.71	0.271	38%
∑ SQDG		1.74	0.439	25%

Notes.

^aAverage molecular weight.

^bnmol mg⁻¹ of dry weight.

and digalactosyldiacylglycerol as major constituents. The ratio of bilayer-forming DGDG to non- bilayer-forming MGDG may affect the properties of chloroplast membranes by altering the lipid bilayer from hexagonal II to lamellar phases (Demé et al., 2014). SQDG and PG are classified as acidic lipids, with their negative charge at neutral pH. In addition, acidic lipids with negative charge in their head groups also affect the organization of thylakoid membranes. PG is the only phospholipid produced in the chloroplasts and it is usually an essential component in the center of photosystem II (Wada & Murata, 2007). SQDG too has an important function in photosynthesis, although the requirement for this lipid differs among species. PG and SQDG are at least partially functionally redundant, which may be related to maintenance of an anionic charge on the surface of the

Table 2 Amounts of phospholipid and glycolipid molecular species extracted from *S. costatus* ($n = 3$). Molecular weights, standard deviations (SD) and relative standard deviations (% RSD) are also indicated.

Molecular species	MW (Da) ^a	Mean (nmol mg ⁻¹) ^b	SD	% RSD
PE(18:1/16:1)	715	0.03	0.01	30%
PE(18:1/18:1)	743	0.02	0.01	45%
PE(18:1/18:2)	741	0.07	0.02	30%
PE(18:1/18:3)	739	0.17	0.05	29%
PE(18:2/18:3)	737	0.33	0.11	33%
PE(18:3/18:3)	735	0.22	0.07	31%
PG(16:0/16:0)	722	0.03	0.00	11%
PG(16:1/16:0)	720	0.03	0.00	4%
PG(18:1/16:0)	748	0.63	0.04	6%
PG(18:2/16:0)	746	0.37	0.03	9%
PG(18:3/16:0)	744	0.30	0.01	5%
PG(18:4/16:0)	742	0.01	0.00	4%
PG(16:1/18:1)	746	0.12	0.01	7%
PG(16:1/18:2)	744	0.09	0.01	15%
PG(16:1/18:3)	742	0.31	0.01	5%
PG(18:1/18:1)	774	0.01	0.00	21%
PG(18:1/18:2)	772	0.01	0.00	16%
PG(18:3/18:1)	770	0.01	0.00	9%
PG(18:3/18:2)	768	0.01	0.00	24%
PG(18:3/18:3)	766	0.01	0.00	32%
PC(16:0/18:2)	758	0.01	0.00	9%
PC(16:0/18:3)	756	0.07	0.02	24%
PC(18:1/18:3)	782	0.07	0.02	33%
PC(18:2/18:3)	780	0.23	0.04	18%
MGDG(18:3/16:3)	746	0.15	0.06	41%
MGDG(18:3/16:4)	744	3.17	0.37	12%
DGDG(16:0_18:1) ^c	918	0.09	0.01	11%
DGDG(18:2/16:0)	916	0.08	0.00	1%
DGDG(18:3/16:0)	914	0.13	0.01	6%
DGDG(16:1/18:1)	916	0.10	0.01	15%
DGDG(16:1_18:2) ^c	914	0.08	0.02	22%
DGDG(18:3/16:1)	912	0.18	0.03	18%
DGDG(18:1/16:2)	914	0.06	0.01	8%
DGDG(18:2/16:2)	912	0.08	0.01	13%
DGDG(18:3/16:2)	910	0.18	0.03	19%
DGDG(18:1/16:3)	912	0.07	0.01	18%
DGDG(18:2/16:3)	910	0.12	0.02	19%
DGDG(18:3/16:3)	908	0.31	0.03	9%
DGDG(16:4/18:2)	908	0.02	0.00	18%
DGDG(16:4/18:3)	906	0.20	0.02	12%

(continued on next page)

Table 2 (continued)

Molecular species	MW (Da) ^a	Mean (nmol mg ⁻¹) ^b	SD	% RSD
DGDG(18:3/18:1)	940	0.02	0.01	70%
DGDG(18:3/18:2)	938	0.07	0.02	32%
DGDG(18:3/18:3)	936	0.13	0.03	22%
SQDG(32:0)	795	0.48	0.12	25%
SQDG(32:1)	793	0.07	0.01	7%
SQDG(34:0)	823	0.06	0.00	9%
SQDG(34:1)	821	0.92	0.13	14%
SQDG(34:2)	819	0.49	0.08	17%
SQDG(34:3)	817	1.38	0.13	9%
SQDG(34:4)	815	0.15	0.00	3%
SQDG(36:1)	849	0.05	0.00	6%
SQDG(36:3)	845	0.06	0.01	13%
SQDG(36:4)	843	0.05	0.01	15%
SQDG(36:6)	839	0.13	0.01	9%
∑ PE		0.84	0.26	31%
∑ PG		1.94	0.11	6%
∑ PC		0.38	0.07	20%
∑ MGDG		3.32	0.42	13%
∑ DGDG		1.96	0.07	3%
∑ SQDG		3.84	0.49	13%

Notes.^aAverage molecular weight.^bnmol mg⁻¹ of dry weight.^cThe intensities of the two product ions associated with the fatty acyl chain were equivalent, and thus the preferential regio-chemistry was undetermined in this case.

thylakoid membrane (Apostolova *et al.*, 2008). The amount of phospholipids in microalgae is usually less than that of the glycolipids, with a few exceptions. The main phospholipids are typically phosphatidylcholine, phosphatidylethanolamine, and phosphatidylglycerol. There is a wide variation in the percentages of different found phospholipids in brown algae (Vyssotski *et al.*, 2017; Bergé *et al.*, 1995), for instance. Furthermore, apart from phosphatidylglycerol, phospholipids are occurring in extraplastidial membranes and among them, phosphatidylcholine and phosphatidylethanolamine are usually the most abundant within algae (Li-Beisson *et al.*, 2019), as observed for *N. palea*.

Polar lipid fatty acid determination from polar lipid molecular species

As illustrated in Eqs. (1) and (2), it is possible to deduce the number of moles of each fatty acid, knowing the number of moles of each molecular species for the combination of the whole polar lipid classes. By summing for example all the 16:1, 18:3 or 20:5 from the various polar lipids they belongs to, a profile of fatty acids from polar lipids (PLFAs) can be estimated for the two microalgae (Table 3).

It was thus obtained two very different profiles, in which we find respectively the predominance of 16:1, 20:2 and 20:5, then to a lesser extent 16:0 and 18:1 for the diatom (*N. palea*), and a majority of 16:4 and 18:3, followed by 16:0, 18:1 and 18:2 for the green algae (*S. costatus*). Zhang *et al.* (2020) showed that six different diatom strains exhibited

Table 3 Equivalent of polar lipid fatty acids (PLFAs) amounts from the polar lipidome of *N. palea* (left) and *S. costatus* (right), $n = 5$ and 3 for each microalgae, respectively.

PLFA	Diatom			Green algae		
	Mean (nmol mg ⁻¹) ^b	SD	% RSD	Mean (nmol mg ⁻¹) ^b	SD	% RSD
14:0	0.13	0.06	46%	N.D	N.D	N.D
16:0	1.16	0.38	33%	1.76	0.06	4%
16:1	4.75	1.78	38%	0.94	0.09	9%
16:2	0.19	0.10	50%	0.32	0.03	10%
16:3	0.00	N.D	N.D	0.65	0.06	12%
16:4	0.00	N.D	N.D	3.39	0.10	12%
18:0	0.00	N.D	N.D	N.D	N.D	N.D
18:1	0.85	0.30	35%	1.51	0.13	9%
18:2	0.00	N.D	N.D	1.56	0.16	10%
18:3	0.00	N.D	N.D	6.70	0.20	5%
18:4	0.00	N.D	N.D	0.01	0.00	4%
20:0	0.15	0.06	38%	N.D	N.D	N.D
20:1	0.00	N.D	N.D	N.D	N.D	N.D
20:2	2.66	1.42	53%	N.D	N.D	N.D
20:5	3.59	1.76	49%	N.D	N.D	N.D
22:6	0.11	0.01	11%	N.D	N.D	N.D
∑ SFA (%)	11%	1%	N.D	10%	1%	N.D
∑ MUFA(%)	43%	2%	N.D	15%	1%	N.D
∑ PUFA (%)	46%	2%	N.D	75%	1%	N.D
PUFA/(SFA+MUFA)	0.83	0.05	6%	3.01	0.32	11%

Notes.^bnmol mg⁻¹ of dry weight.

fatty acid compositions typical of the class *Bacillariophyceae*, with a majority of 14:0, 16:0, 16:1, and 20:5. Among these strains, the authors identified *N. palea* HB170, which showed a fatty acid composition in agreement with our observations, although in our study we focused on polar lipids while *Zhang et al. (2020)* determined the total fatty acid content or that derived from triglycerides alone. Regarding green algae, *Sato et al. (1995)* previously reported the occurrence of pinolenic acid (18:3 n -6) and coniferonic acid (18:4 n -3) in the case of *Chlamydomonas reinhardtii*. In our case, we do observe for *S costatus* the presence of 18:3, potentially corresponding to pinolenic acid described earlier, but 18:4, which could be associated with coniferonic acid, was barely detected. Moreover, 18:3 may also correspond to α -linolenic acid (*Kajikawa et al., 2006*). As for 16:4 observed in our green algae extracts, which is typically derived from galactolipids as reported by *Kumari et al. (2013)*, it may correspond to an unusual n -3 PUFA also reported with *Chlamydomonas reinhardtii*. The majority of diatom species (or *Bacillariophyta*) investigated in literature (*Alonso et al., 1998; Abida et al., 2015*) synthesize glycolipids with a prokaryotic structure, confirming our previous observations. The characteristic fatty acids of diatoms from these glycolipids are 14:0, 16:0, 16:1, and 20:5 n -3 or eicosapentaenoic acid, whereas 16:2, 16:3, 16:4 18:0, 18:1, 18:2 or 18:3 fatty acids are in general lower or even absent (*Lang et al., 2011*). The desaturation degree and the amount of C16 fatty acids vary in the different diatom species.

Moreover, 16:3 and 16:4 are only present in glycolipids, when occurring, while 20:5 is found in all lipids, but restricted to *sn*-1 position in glycolipids (Yongmanitchai & Ward, 1993; D'Ippolito et al., 2015; Xu et al., 2010), which was consistent with our observations for both MGDG and DGDG (Table 1). To conclude this section, eicosadienoic acid (20:2 n -6) is a long chain PUFA less frequently observed than eicosapentaenoic in diatoms (Sayanova et al., 2017). This fatty acid can be obtained from Δ 9 elongation of linoleic acid, and could be considered here as a likely specific marker of *N. palea*.

CONCLUSIONS

This study analyzed polar lipids of two freshwater microalgae, *Nitzschia palea* and *Scenedesmus costatus*. The main molecular species associated with glycolipids and phospholipids were characterized, including fragmentation patterns in mass spectrometry for glycolipids. Quantification of these molecular species was also provided. The methodology aimed to supply typical polar lipidome profiles for both “model” diatoms and green algae. The most intense product ion corresponded to the fatty acyl chain at the *sn*-1 position, allowing the determination of the stereospecific distribution of subsequent fatty acids on the glycerol backbone for glycolipids, in addition to phospholipids. Polar lipid molecular species of *N. palea* and *S. costatus* also revealed that MGDG and DGDG contained combinations of SFAs or MUFAs with 20:5 for the diatom, while this C20-PUFA was absent from the green algae. The presence of some specific molecular species, such as MGDG (20:5/20:2) in *N. palea*, could be useful in chemotaxonomy to characterize the evolution of algal community structure as a function of environmental stress occurring *in situ* or reproduced with culture conditions. The same polar lipid analysis proposed in this work can of course be further applied to algal monocultures to monitor the physiological effects, on either cytoplasmic membranes or thylakoids, of varying physical (light or temperature), physicochemical (pH, nutrients) or chemical (micropollutants) factors.

ACKNOWLEDGEMENTS

The authors would like to thank for technical Sylvia Moreira, Gwilherm Jan and Jacky Vedrenne for laboratory assistance regarding microalgae cultures. The authors also thank the Aquatic Vegetation Pole of the ISC XPO (<https://doi.org/10.17180/BREY-MR38>) of the UR EABX for providing the laboratories and equipment necessary to perform the analyses in this study.

ADDITIONAL INFORMATION AND DECLARATIONS

Funding

This study has been carried out with financial support from the French National Research Agency (ANR) in the frame of the Investments for the future Programme, within the Cluster of Excellence COTE (ANR-10-LABX-45). The funders had no role in study design, data collection and analysis, decision to publish, or preparation of the manuscript.

Grant Disclosures

The following grant information was disclosed by the authors:

The French National Research Agency (ANR) in the frame of the Investments for the future Programme, within the Cluster of Excellence COTE: ANR-10-LABX-45.

Competing Interests

The authors declare that there are no competing interests.

Author Contributions

- Nicolas Mazzella conceived and designed the experiments, performed the experiments, analyzed the data, prepared figures and/or tables, authored or reviewed drafts of the article, and approved the final draft.
- Mariem Fadhlaoui conceived and designed the experiments, performed the experiments, authored or reviewed drafts of the article, and approved the final draft.
- Aurélie Moreira performed the experiments, authored or reviewed drafts of the article, and approved the final draft.
- Soizic Morin conceived and designed the experiments, authored or reviewed drafts of the article, and approved the final draft.

Data Deposition

The following information was supplied regarding data availability:

The raw data is available [Supplemental Files](#).

Supplemental Information

Supplemental information for this article can be found online at <http://dx.doi.org/10.7717/peerj-achem.27#supplemental-information>.

REFERENCES

- Abida H, Dolch LJ, Meï C, Villanova V, Conte M, Block MA, Finazzi G, Bastien O, Tirichine L, Bowler C, Rébeillé F, Petroutsos D, Jouhet J, Maréchal E. 2015. Membrane glycerolipid remodeling triggered by nitrogen and phosphorus starvation in *Phaeodactylum tricornutum*. *Plant Physiology* **167**(1):118–136 DOI 10.1104/pp.114.252395.
- Alonso DL, Belarbi E-H, Rodríguez-Ruiz J, Segura CI, Giménez A. 1998. Acyl lipids of three microalgae. *Phytochemistry* **47**(8):1473–1481 DOI 10.1016/S0031-9422(97)01080-7.
- Apostolova EL, Domonkos I, Dobrikova AG, Sallai A, Bogos B, Wada H, Gombos Z, Taneva SG. 2008. Effect of phosphatidylglycerol depletion on the surface electric properties and the fluorescence emission of thylakoid membranes. *Journal of Photochemistry and Photobiology B: Biology* **91**(1):51–57 DOI 10.1016/j.jphotobiol.2008.02.002.
- Arts MT, Ackman RG, Holub BJ. 2001. Essential fatty acids in aquatic ecosystems: a crucial link between diet and human health and evolution. *Canadian Journal of Fisheries and Aquatic Sciences* **58**:122–137 DOI 10.1139/f00-224.

- Bergé J-P, Gouygou J-P, Dubacq J-P, Durand P. 1995.** Reassessment of lipid composition of the diatom. *Skeletonema costatum*. *Phytochemistry* **39**(5):1017–1021 DOI [10.1016/0031-9422\(94\)00156-N](https://doi.org/10.1016/0031-9422(94)00156-N).
- Block MA, Dorne AJ, Joyard J, Douce R. 1983.** Preparation and characterization of membrane fractions enriched in outer and inner envelope membranes from spinach chloroplasts. II. Biochemical characterization. *The Journal of Biological Chemistry* **258**(21):13281–13286 DOI [10.1016/S0021-9258\(17\)44113-5](https://doi.org/10.1016/S0021-9258(17)44113-5).
- Brett MT, Müller-Navarra DC. 1997.** The role of highly unsaturated fatty acids in aquatic foodweb processes. *Freshwater Biology* **38**:483–499 DOI [10.1046/j.1365-2427.1997.00220.x](https://doi.org/10.1046/j.1365-2427.1997.00220.x).
- Choi K, Nakhost Z, Bárzana E, Karel M. 1987.** Lipid content and fatty acid composition of green algae *Scenedesmus obliquus* grown in a constant cell density apparatus. *Food Biotechnology* **1**:117–128 DOI [10.1080/08905438709549660](https://doi.org/10.1080/08905438709549660).
- Coniglio D, Bianco M, Ventura G, Calvano CD, Losito I, Cataldi TRI. 2021.** Lipidomics of the edible brown alga wakame (*Undaria pinnatifida*) by liquid chromatography coupled to electrospray ionization and tandem mass spectrometry. *Molecules* **26**(15):4480 DOI [10.3390/molecules26154480](https://doi.org/10.3390/molecules26154480).
- Cutignano A, Luongo E, Nuzzo G, Pagano D, Manzo E, Sardo A, Fontana A. 2016.** Profiling of complex lipids in marine microalgae by UHPLC/tandem mass spectrometry. *Algal Research* **17**:348–358 DOI [10.1016/j.algal.2016.05.016](https://doi.org/10.1016/j.algal.2016.05.016).
- Da Costa E, Silva J, Mendonça SH, Abreu MH, Domingues MR. 2016.** Lipidomic approaches towards deciphering glycolipids from microalgae as a reservoir of bioactive lipids. *Marine Drugs* **14**(5):101 DOI [10.3390/md14050101](https://doi.org/10.3390/md14050101).
- Dauta A. 1982.** Conditions de développement du phytoplancton. Etude comparative du comportement de huit espèces en culture. II: Rôle des nutriments: assimilation et stockage intracellulaire. *Annales de Limnologie—International Journal of Limnology* **18**:263–292 DOI [10.1051/limn/1982014](https://doi.org/10.1051/limn/1982014).
- Degraeve-Guilbault C, Bréhélin C, Haslam R, Sayanova O, Marie-Luce G, Jouhet J, Corellou F. 2017.** Glycerolipid characterization and nutrient deprivation-associated changes in the green picoalga *Ostreococcus tauri*. *Plant Physiology* **173**(4):2060–2080 DOI [10.1104/pp.16.01467](https://doi.org/10.1104/pp.16.01467).
- Demaiilly F, Elfeky I, Malbezin L, Le Guédard M, Eon M, Bessoule J-J, Feurtet-Mazel A, Delmas F, Mazzella N, Gonzalez P, Morin S. 2019.** Impact of diuron and S-metolachlor on the freshwater diatom *Gomphonema gracile*: complementarity between fatty acid profiles and different kinds of ecotoxicological impact-endpoints. *Science of the Total Environment* **688**:960–969 DOI [10.1016/j.scitotenv.2019.06.347](https://doi.org/10.1016/j.scitotenv.2019.06.347).
- Demé B, Cataye C, Block MA, Maréchal E, Jouhet J. 2014.** Contribution of galactoglycerolipids to the 3-dimensional architecture of thylakoids. *FASEB Journal* **28**(8):3373–3383 DOI [10.1096/fj.13-247395](https://doi.org/10.1096/fj.13-247395).
- D’Ippolito G, Sardo A, Paris D, Vella FM, Adelfi MG, Botte P, Gallo C, Fontana A. 2015.** Potential of lipid metabolism in marine diatoms for biofuel production. *Biotechnology for Biofuels* **8**:28 DOI [10.1186/s13068-015-0212-4](https://doi.org/10.1186/s13068-015-0212-4).

- Fournier F, Remaud B, Blasco T, Tabet JC. 1993.** Ion-dipole complex formation from deprotonated phenol fatty acid esters evidenced by using gas-phase labeling combined with tandem mass spectrometry. *Journal of the American Society for Mass Spectrometry* **4(4)**:343–351 DOI [10.1016/1044-0305\(93\)85057-5](https://doi.org/10.1016/1044-0305(93)85057-5).
- Giroud C, Gerber A, Eichenberger W. 1988.** Lipids of *Chlamydomonas reinhardtii*. Analysis of molecular species and intracellular site(s) of biosynthesis. *Plant and Cell Physiology* **29(4)**:587–595.
- Guschina IA, Harwood JL. 2006.** Lipids and lipid metabolism in eukaryotic algae. *Progress in Lipid Research* **45(2)**:160–186 DOI [10.1016/j.plipres.2006.01.001](https://doi.org/10.1016/j.plipres.2006.01.001).
- Herrero M, Vicente MJ, Cifuentes A, Ibáñez E. 2007.** Characterization by high-performance liquid chromatography/electrospray ionization quadrupole time-of-flight mass spectrometry of the lipid fraction of *Spirulina platensis* pressurized ethanol extract. *Rapid Communications in Mass Spectrometry: RCM* **21(11)**:1729–1738 DOI [10.1002/rcm.3017](https://doi.org/10.1002/rcm.3017).
- Hsu F-F, Turk J. 2000.** Charge-remote and charge-driven fragmentation processes in diacyl glycerophosphoethanolamine upon low-energy collisional activation: a mechanistic proposal. *Journal of the American Society for Mass Spectrometry* **11(10)**:892–899 DOI [10.1016/S1044-0305\(00\)00159-8](https://doi.org/10.1016/S1044-0305(00)00159-8).
- Hsu F-F, Turk J. 2001.** Studies on phosphatidylglycerol with triple quadrupole tandem mass spectrometry with electrospray ionization: fragmentation processes and structural characterization. *Journal of the American Society for Mass Spectrometry* **12(9)**:1036–1043 DOI [10.1016/S1044-0305\(01\)00285-9](https://doi.org/10.1016/S1044-0305(01)00285-9).
- Hsu F-F, Turk J. 2009.** Electrospray ionization with low-energy collisionally activated dissociation tandem mass spectrometry of glycerophospholipids: mechanisms of fragmentation and structural characterization. *Journal of Chromatography B* **877(26)**:2673–2695 DOI [10.1016/j.jchromb.2009.02.033](https://doi.org/10.1016/j.jchromb.2009.02.033).
- Huang Q, Lei H, Dong M, Tang H, Wang Y. 2019.** Quantitative analysis of 10 classes of phospholipids by ultrahigh-performance liquid chromatography tandem triple-quadrupole mass spectrometry. *Analyst* **144(13)**:3980–3987 DOI [10.1039/C9AN00676A](https://doi.org/10.1039/C9AN00676A).
- Jouhet J, Lupette J, Clerc O, Magneschi L, Bedhomme M, Collin S, Roy S, Maréchal E, Rébeillé F. 2017.** LC-MS/MS versus TLC plus GC methods: consistency of glycerolipid and fatty acid profiles in microalgae and higher plant cells and effect of a nitrogen starvation. *PLOS ONE* **12(8)**:e0182423 DOI [10.1371/journal.pone.0182423](https://doi.org/10.1371/journal.pone.0182423).
- Kajikawa M, Yamato KT, Kohzu Y, Shoji S, Matsui K, Tanaka Y, Sakai Y, Fukuzawa H. 2006.** A front-end desaturase from *Chlamydomonas reinhardtii* produces pinolenic and coniferonic acids by omega13 desaturation in methylotrophic yeast and tobacco. *Plant & Cell Physiology* **47(1)**:64–73 DOI [10.1093/pcp/pci224](https://doi.org/10.1093/pcp/pci224).
- Kelly JR, Scheibling RE. 2012.** Fatty acids as dietary tracers in benthic food webs. *Marine Ecology Progress Series* **446**:1–22 DOI [10.3354/meps09559](https://doi.org/10.3354/meps09559).
- Kumari P, Bijo AJ, Mantri VA, Reddy CR, Jha B. 2013.** Fatty acid profiling of tropical marine macroalgae: an analysis from chemotaxonomic and nutritional perspectives. *Phytochemistry* **86**:44–56 DOI [10.1016/j.phytochem.2012.10.015](https://doi.org/10.1016/j.phytochem.2012.10.015).

- Lang I, Hodac L, Friedl T, Feussner I. 2011.** Fatty acid profiles and their distribution patterns in microalgae: a comprehensive analysis of more than 2000 strains from the SAG culture collection. *BMC Plant Biology* **11**:124–124 DOI [10.1186/1471-2229-11-124](https://doi.org/10.1186/1471-2229-11-124).
- Li L, Chang M, Tao G, Wang X, Liu Y, Liu R, Jin Q, Wang X. 2016.** Analysis of phospholipids in *Schizochytrium* sp. S31 by using UPLC-Q-TOF-MS. *Analytical Methods* **8**(4):763–770 DOI [10.1039/C5AY02795K](https://doi.org/10.1039/C5AY02795K).
- Li X, He Q, Hou H, Zhang S, Zhang X, Zhang Y, Wang X, Han L, Liu K. 2018.** Targeted lipidomics profiling of marine phospholipids from different resources by UPLC-Q-Exactive Orbitrap/MS approach. *Journal of Chromatography B* **1096**:107–112 DOI [10.1016/j.jchromb.2018.08.018](https://doi.org/10.1016/j.jchromb.2018.08.018).
- Li-Beisson Y, Thelen JJ, Fedosejevs E, Harwood JL. 2019.** The lipid biochemistry of eukaryotic algae. *Progress in Lipid Research* **74**:31–68 DOI [10.1016/j.plipres.2019.01.003](https://doi.org/10.1016/j.plipres.2019.01.003).
- Matyash V, Liebisch G, Kurzchalia TV, Shevchenko A, Schwudke D. 2008.** Lipid extraction by methyl-tert-butyl ether for high-throughput lipidomics. *Journal of Lipid Research* **49**(5):1137–1146 DOI [10.1194/jlr.D700041-JLR200](https://doi.org/10.1194/jlr.D700041-JLR200).
- Mazzella N, Fadhlaoui M, Moreira A, Morin S. 2023a.** Molecular species composition of polar lipids from two microalgae *Nitzschia palea* and *Scenedesmus costatus* using HPLC-ESI-MS/MS. Available at <https://doi.org/10.26434/chemrxiv-2022-7cjgc-v4>.
- Mazzella N, Molinet J, Syakti AD, Bertrand J-C, Doumenq P. 2007.** Assessment of the effects of hydrocarbon contamination on the sedimentary bacterial communities and determination of the polar lipid fraction purity: relevance of intact phospholipid analysis. *Marine Chemistry* **103**(3):304–317 DOI [10.1016/j.marchem.2006.09.007](https://doi.org/10.1016/j.marchem.2006.09.007).
- Mazzella N, Molinet J, Syakti AD, Dodi A, Bertrand J-C, Doumenq P. 2005.** Use of electrospray ionization mass spectrometry for profiling of crude oil effects on the phospholipid molecular species of two marine bacteria. *Rapid Communications in Mass Spectrometry* **19**(23):3579–3588 DOI [10.1002/rcm.2231](https://doi.org/10.1002/rcm.2231).
- Mazzella N, Molinet J, Syakti AD, Dodi A, Doumenq P, Artaud J, Bertrand J-C. 2004.** Bacterial phospholipid molecular species analysis by ion-pair reversed-phase HPLC/ESI/MS. *Journal of Lipid Research* **45**(7):1355–1363 DOI [10.1194/jlr.D300040-JLR200](https://doi.org/10.1194/jlr.D300040-JLR200).
- Mazzella N, Moreira A, Eon M, Médina A, Millan-Navarro D, Creusot N. 2023b.** Hydrophilic interaction liquid chromatography coupled with tandem mass spectrometry method for quantification of five phospholipid classes in various matrices. *Methods* **10**:102026.
- Mizusawa N, Wada H. 2012.** The role of lipids in photosystem II. *Biochimica Et Biophysica Acta (BBA)—Bioenergetics* **1817**(1):194–208 DOI [10.1016/j.bbabi.2011.04.008](https://doi.org/10.1016/j.bbabi.2011.04.008).
- Pi J, Wu X, Feng Y. 2016.** Fragmentation patterns of five types of phospholipids by ultra-high-performance liquid chromatography electrospray ionization quadrupole time-of-flight tandem mass spectrometry. *Analytical Methods* **8**(6):1319–1332 DOI [10.1039/C5AY00776C](https://doi.org/10.1039/C5AY00776C).

- Rimet F, Chardon C, Lainé L, Bouchez A, Domaizon I, Guillard J, Jacquet S. 2018.** Thonon Culture Collection—TCC—a freshwater microalgae collection. Available at <https://doi.org/10.15454/UQEMVW>, Portail Data Inra, V1.
- Sanina NM, Goncharova SN, Kostetsky EY. 2004.** Fatty acid composition of individual polar lipid classes from marine macrophytes. *Phytochemistry* **65**(6):721–730 DOI 10.1016/j.phytochem.2004.01.013.
- Sato N, Sonoike K, Tsuzuk M, Kawaguchi A. 1995.** Impaired photosystem II in a mutant of *Chlamydomonas reinhardtii* defective in sulfoquinovosyl diacylglycerol. *European Journal of Biochemistry* **234**(1):16–23 DOI 10.1111/j.1432-1033.1995.016_c.x.
- Sayanova O, Mimouni V, Ulmann L, Morant-Manceau A, Pasquet V, Schoefs B, Napier JA. 2017.** Modulation of lipid biosynthesis by stress in diatoms. *Philosophical Transactions of the Royal Society B: Biological Sciences* **372**(1728):20160407 DOI 10.1098/rstb.2016.0407.
- Taipale S, Strandberg U, Peltomaa E, Galloway AWE, Ojala A, Brett MT. 2013.** Fatty acid composition as biomarkers of freshwater microalgae: analysis of 37 strains of microalgae in 22 genera and in seven classes. *Aquatic Microbial Ecology* **71**:165–178 DOI 10.3354/ame01671.
- Tatituri RVV, Brenner MB, Turk J, Hsu F-F. 2012.** Structural elucidation of diglycosyl diacylglycerol and monoglycosyl diacylglycerol from *Streptococcus pneumoniae* by multiple-stage linear ion-trap mass spectrometry with electrospray ionization. *Journal of Mass Spectrometry* **47**(1):115–123 DOI 10.1002/jms.2033.
- Vyssotski M, Lagutin K, MacKenzie A, Mitchell K, Scott D. 2017.** Phospholipids of New Zealand edible brown algae. *Lipids* **52**(7):629–639 DOI 10.1007/s11745-017-4266-x.
- Wada H, Murata N. 2007.** The essential role of phosphatidylglycerol in photosynthesis. *Photosynthesis Research* **92**:205–215 DOI 10.1007/s11120-007-9203-z.
- Xu J, Chen D, Yan X, Chen J, Zhou C. 2010.** Global characterization of the photosynthetic glycerolipids from a marine diatom *Stephanodiscus* sp. by ultra performance liquid chromatography coupled with electrospray ionization-quadrupole-time of flight mass spectrometry. *Analytica Chimica Acta* **663**(1):60–68 DOI 10.1016/j.aca.2010.01.026.
- Yingbo Z, Ximan K, Yajuan W, Huajun S, Shujuan J. 2021.** Comprehensive analysis of phospholipids and glycerol glycolipids in green pepper by ultra-performance liquid chromatography/quadrupole time-of-flight mass spectrometry. *Rapid Communications in Mass Spectrometry* **35**(18):e9146.
- Yongmanitchai W, Ward OP. 1993.** Positional distribution of fatty acids, and molecular species of polar lipids, in the diatom *Phaeodactylum tricornutum*. *Journal of General Microbiology* **139**(3):465–472 DOI 10.1099/00221287-139-3-465.
- Zhang L, Hu F, Wan X, Pan Y, Hu H. 2020.** Screening of high temperature-tolerant oleaginous diatoms. *Journal of Microbiology and Biotechnology* **30**(7):1072–1081 DOI 10.4014/jmb.2002.02053.
- Zulfiqar S, Sharif S, Saeed M, Tahir A. 2003.** Role of carotenoids in photosynthesis. In: *Photosynthesis. Advances in photosynthesis and respiration*. Vol. 10. Dordrecht: Springer.

Zulu NN, Zienkiewicz K, Vollheyde K, Feussner I. 2018. Current trends to comprehend lipid metabolism in diatoms. *Progress in Lipid Research* **70**:1–16
DOI [10.1016/j.plipres.2018.03.001](https://doi.org/10.1016/j.plipres.2018.03.001).